

**CHAPTER 7: ENVIRONMENTAL MAGNETISM AND  
GEOCHEMICAL STUDIES**

## **7.1 Environmental Magnetic Studies**

Magnetic property of the sediment quantifies omnipresent occurrence of iron oxides formed in situ or transported through various processes. The application of environmental magnetic studies thus have been widely accepted for their role in all environments viz., climate (Kukla et al., 1988; An et al., 1991; Basavaiah and Khadkikar, 2004; Deotare et al., 2004; Juyal et al., 2004; Cui et al., 2005; Pant et al., 2005; Sukanuma et al., 2009; Warrier and Shankar, 2009; Ao, 2010; Basavaiah, 2011); sediment transportation pathways (Ellwood et al., 2006; Rotman et al., 2008; Alagarsamy, 2009; Dessai et al., 2009; Cioppa et al., 2010; Liu et al., 2010b; Wang et al., 2010a); transporting medium (Thompson and Oldfield, 1986; Verosub and Roberts, 1995; Dekkers, 1997; Maher and Thompson, 1999; Evans and Heller, 2003; Basavaiah and Khadkikar, 2004; Sangode et al., 2007); grain size distribution (Thompson and Morton, 1979; King et al., 1982; Oldfield and Yu, 1994; Peters and Dekkers, 2003; Booth et al., 2005; Booth et al., 2008); depositional settings such as aeolian- loess (Heller and Tung-sheng, 1986; Kukla et al., 1988; Begét et al., 1990; An et al., 1991; Heller et al., 1991; Beer et al., 1993; Verosub et al., 1993), lacustrine environment (King et al., 1982; Snowball, 1993; Zhu et al., 2003), marginal marine environment (Rajshekhar et al., 1991; Liu et al., 2003; Pattan et al., 2008; Rotman et al., 2008; Alagarsamy, 2009; Liu et al., 2010a; Wang et al., 2010b) and fluvial environment (Thompson and Morton, 1979; Cui et al., 2005; Sangode et al., 2007; Sinha et al., 2007a; Ao, 2010).

### **7.1.1 Sample and Analysis**

The magnetic characterisation of sediment samples were carried out on three aspects viz., 1. Measurement of magnetic susceptibility carried out at a 2 cm sample interval (In all 401 samples were analysed); 2. Measurement of Saturation Isothermal Remnant Magnetization (SIRM) carried out at 2 cm interval for fine facies and 10 cm interval for coarse sedimentary facies (In all 276 samples were analysed) and 3. Separation of Ferrimagnetic Mineral Concentration (FMC) carried

out for 10 cm interval, however, significant sediment units were further analysed at 2 cm interval (In all 205 samples were analysed) were also carried out.

### **7.1.2 Sample Preparation for Magnetic Studies**

For magnetic measurements bulk samples collected from field was packed tightly in 10 cc plastic bottles (Standard bottle for measurement). The weight of empty plastic bottles and plastic bottles tightly packed with sample were recorded. The magnetic measurements were carried out in the Environmental Magnetic Laboratory at Indian Institute of Geomagnetism Panvel, Mumbai. For separation of FMC, 2 sets of 10 grams of representative samples were separated and packed in aluminium foil. One set was used for the FMC separation and another set was preserved and used for cross checking of the recorded FMC.

### **7.1.3 Environmental Magnetic Measurement**

The samples were measured for mainly three parameters: 1. Low frequency volume susceptibility ( $\kappa_{lf}$ ), 2. High frequency volume susceptibility ( $\kappa_{hf}$ ) and 3. Saturation Isothermal Remnant Magnetization (SIRM). Mass specific Susceptibility ( $\chi_{lf}$ ) and Frequency dependent of Susceptibility ( $\chi_{fd}$ ) were further calculated. As the measurements are simple and fast, the magnetic susceptibility often ideal in reconnaissance studies, where a large sample set are to be analysed (Thompson and Oldfield, 1986; Verosub and Roberts, 1995; Dealing et al., 1996; Evans and Heller, 2003; Basavaiah, 2011).

The low field magnetic susceptibility is the most fundamental and extensively used parameter at room temperature. The mass normalized susceptibility ( $\chi_{lf}$ ) is a first order estimate of ferromagnetic concentration and is an important parameter when used with other parameters. Another extremely important susceptibility parameter is Frequency dependency ( $\chi_{fd}$ ), is the difference in susceptibility observed when the instrument is used at two different frequencies. This is particularly important in detecting the sediment magnetic

mineral grain size domain. Table 7- summarizes the parameters, its units and descriptions used in the study.

Table 7-: Parameters, units and descriptions used for the environmental magnetic studies

Parameter	Unit	Description
High frequency volume susceptibility ( $\kappa_{hf}$ )	Dimensionless	Volume susceptibility measured at high frequency of 3904 Hz with field strength 113 A/m. Defined as $\kappa=M/H$ ; M is volume magnetization induced, H- is intensity of field.
Low frequency volume susceptibility ( $\kappa_{lf}$ )	Dimensionless	Volume susceptibility measured at high frequency of 976 Hz with field strength 113 A/m. Defined as $\kappa=M/H$ ; M is volume magnetization induced, H- is intensity of field
Mass specific Susceptibility ( $\chi_{lf}$ )	$\times 10^{-6} \text{ m}^3\text{kg}^{-1}$	Is measured as the ratio of low frequency volume susceptibility to density. $\div = \kappa/\tilde{n}$
Frequency dependent of Susceptibility ( $\chi_{fd} \%$ )	Percentage	Percentage of variation in $\div$ between low frequency and high frequency.
Saturation isothermal remnant magnetization (SIRM)	$\times 10^{-5} \text{ Am}^2\text{kg}^{-1}$	Measured as the highest volume of magnetic remanence that can be produced in a sample by application of very high field. SIRM relate to both mineral type and concentration.

Laboratory measurement for  $\kappa_{lf}$  and  $\kappa_{hf}$  were carried out using Multi-function automated MFK-1 Kapabridge (Agico AGICO Inc. Brno, Czech Republic) Magnetic Susceptibility meter having a high sensitivity of  $2 \times 10^{-6}$  (SI unit) at optimum conditions. The measurements were done at two different frequencies 976 Hz and 3904 Hz with field strength of 113 A/m. The SIRM is measured after exposing the sample to a high saturating magnetic field of 1 tesla. The intensity of Isothermal Remnant Magnetization can be measured at this stage. Initially the

samples were exposed to a high magnetic field of 1.00 tesl in a Pulse Magnetiser and the saturation isothermal remanence is measured using a Molspin Magnetometer.

#### 7.1.3.1 Calculation of Mass Specific Susceptibility

Environmental studies often measure magnetic susceptibility on materials, which due to their nature or preparation have widely different bulk densities. This makes comparison of  $\kappa$  values difficult. Therefore single sample susceptibility is not normally expressed on volumetric basis ( $\kappa$ ), but not on dry mass. In order to obtain mass specific susceptibility, the corrected  $\kappa$  value is divided by the bulk density of the sample.

Mass specific magnetic susceptibility ( $\chi$ ) is expressed as:

$$\chi = \kappa/\rho$$

Where,

$\kappa$  is the volume susceptibility

$\rho$  is sample density

#### 7.1.3.2 Calculation of Frequency Dependent Susceptibility

The measurement made at two frequencies is used to detect the presence of ultrafine (<0.03  $\mu\text{m}$ ) super paramagnetic minerals occurring as crystals. The procedure involves making a  $\kappa$  reading in magnetic fields created at two different frequencies (976 Hz and 3904 Hz). Sample comprising of ultrafine minerals will show lower values when measured at high frequencies. The Kapabridge sensor allows the choice of low frequency (LF) or high frequency (HF) range. Frequency dependent susceptibility may be expressed either as a percentage of the original LF values or as a mass specific frequency dependent susceptibility values for frequencies of the sensor. The calculations are simple expression of the same data in relative and absolute forms analogous to the type and concentration of magnetic minerals respectively. Percentage frequency dependent susceptibility ( $\kappa_{fd\%}$  or more commonly  $\chi_{fd\%}$ ) is:

$$\chi_{fd}\% = \frac{\kappa_{lf} - \kappa_{hf}}{\kappa_{lf}} \times 100$$

Where

$\kappa_{lf}$  is the corrected reading at low frequency

$\kappa_{hf}$  is the corrected reading at high frequency

#### 7.1.4 Ferrimagnetic Mineral Concentration

A 10 gram of sample is resampled after conning and quartering of the bulk sample. The method adopted for separation ferrimagnetic mineral is that used for preparation for Frantz magnetic separator. The resampled fraction is taken in parts and spread over an aluminium foil. A hand magnet covered with a thin plastic film is repeatedly moved over the sediment at a certain distance. During this process, the magnetic minerals fly and stick to the magnet. The magnetic minerals are then transferred to another aluminium foil. The experiment is repeatedly done for several iterations till no grain is observed attracted towards the magnet. This confirms all the magnetic minerals are separated from the bulk sample. The magnetic mineral fractions are further enriched by a similar process removing other grains that have got attracted because of electrostatic charge generated on the nonmagnetic mineral. The ferromagnetic minerals are further observed under a binocular microscope for confirmation. Weight of both magnetic and nonmagnetic materials were measured and converted to weight percentage values for the further analysis. Similar studies were used to infer the flood events from a vertical section in Mahi River basin (Sant et al., 2006).

#### 7.1.5 Results and Discussion

The mineral magnetic properties namely, Low-frequency Magnetic susceptibility ( $\chi_{lf}$ ) and Saturation Isothermal Remnant Magnetisation (SIRM) are plotted along the depth profile and further used for different bivariate scatter plots. Frequency dependent susceptibility ( $\chi_{fd}$ ) is calculated for the sequence shows a very low dependency (less than 5%) which indicate absence of ultrafine magnetic grains and in turn suggest fresh sediments as a consequence  $\chi_{fd}$  record is

not considered for interpretation. The overall characteristic of magnetic mineral in the fluvial sediment is tabulated in Table 7-.

The plot of  $\chi_{lf}$  against SIRM record shows contribution of ferrimagnetic minerals is proportional to concentration of all remanence carrying minerals (Figure 7-). The plot of  $\chi_{lf}$  and SIRM record along depth profile of the sediment sequence under study also show overall similar variation along the depth of the sequence (Figure 7-). The significant variation in values of  $\chi_{lf}$  is recorded in Figure 7-.

Table 7-: The mineral magnetic properties for Late Holocene flood plain sediment along depth profile.

	Units	No. of samples	Minimum	Maximum	Mean	Standard deviation
$\chi_{lf}$	$10^{-6} \text{ m}^3 \text{ Kg}^{-1}$ $10^{-5} \text{ Am}^2$	401	216	1693	598	205
SIRM	$\text{Kg}^{-1}$	276	563.3683	18361.03	6965.747	2438

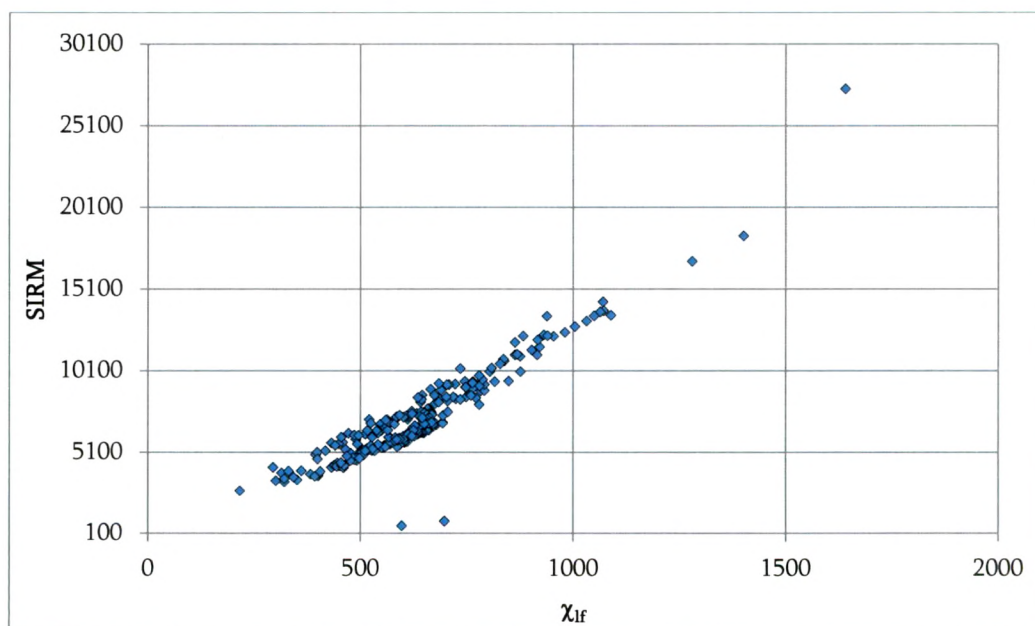


Figure 7-: Plot of  $\chi_{lf}$  against SIRM

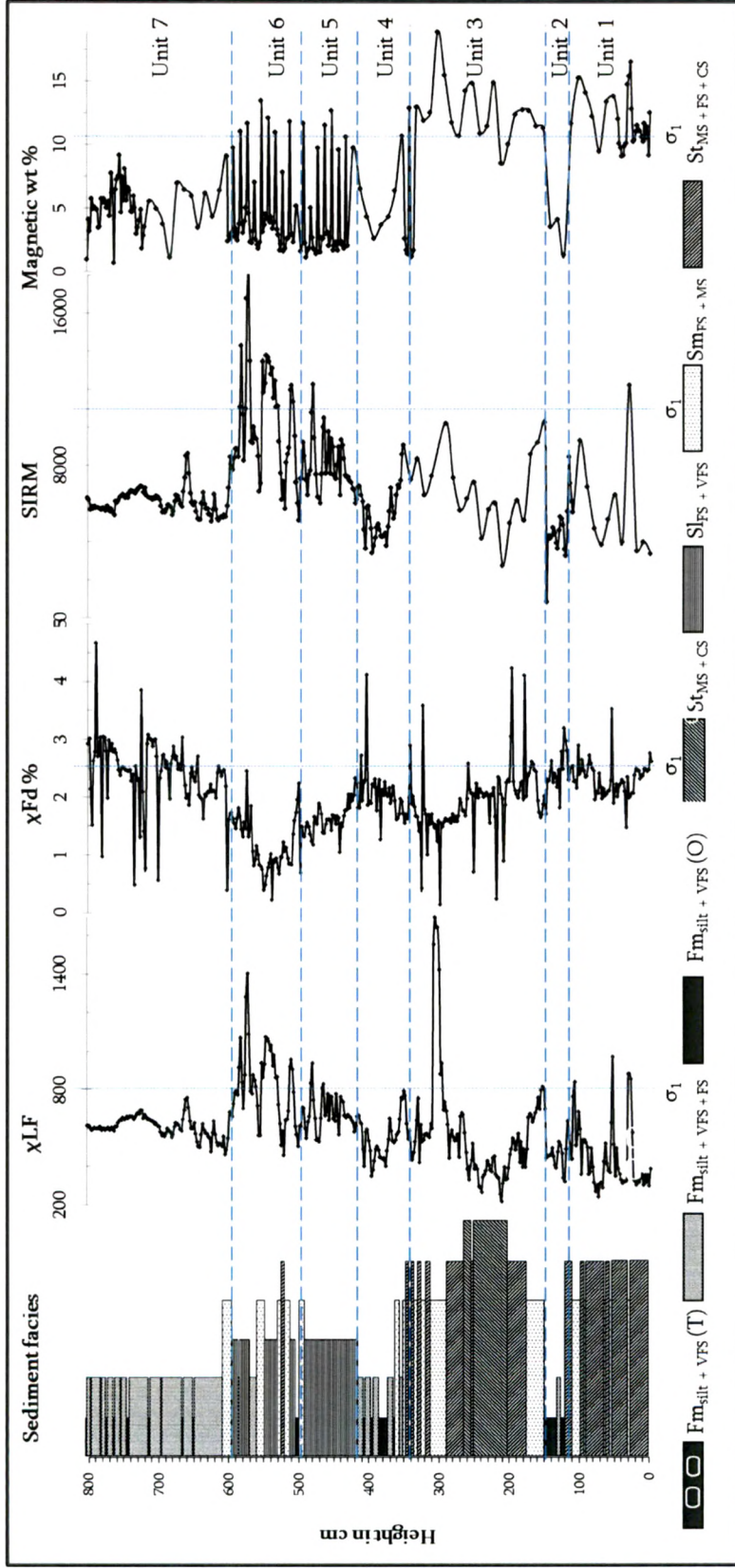


Figure 7:- Depth wise variation of magnetic parameters from the Uchediya section.



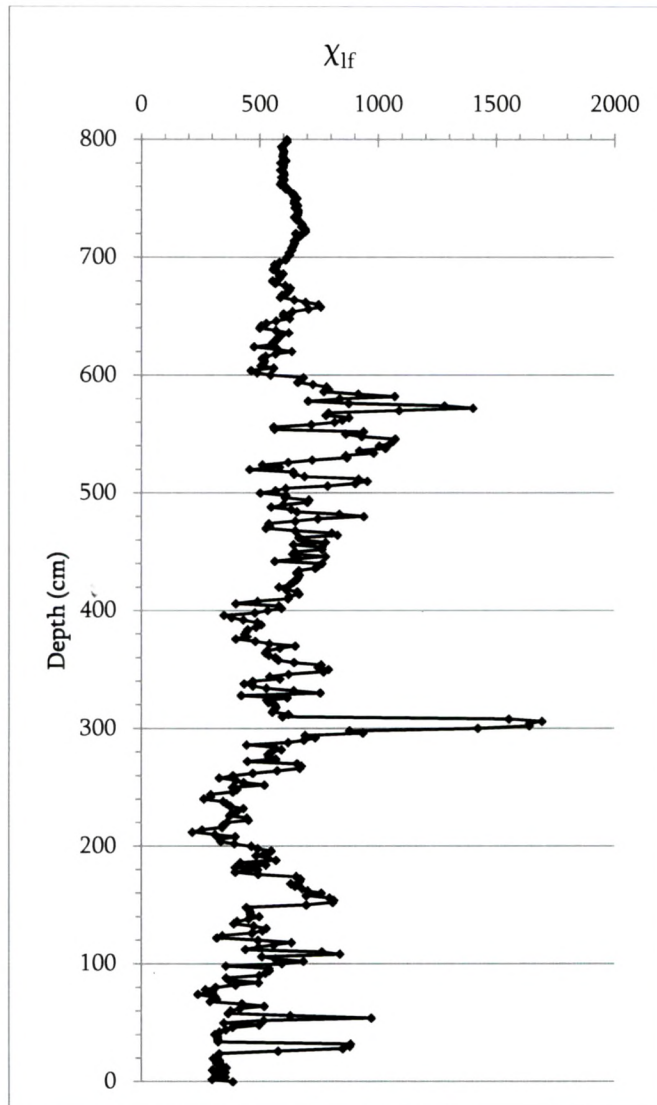


Figure 7-: Depth wise variation of  $\chi_{If}$  values for Uchediya sequence

In Figure 7-, the mean value of  $\chi_{If}$  between 0 cm and 148 cm is 452 SI units with 3 significant peaks at 32 cm (883 SI units), 54 cm (970 SI unit) and 108 cm (838 SI units). The values of  $\chi_{If}$  shows consistent decrease from 152 cm (808 SI unit) to 212 cm ( 216 SI units) thereafter the values show gradual increase up to 292 cm (734 SI units) with 3 minor peaks at 222 cm (454 SI units), 252 cm (520 SI units) and 268 cm (677 SI units). The  $\chi_{If}$  values show a sharp rise from 292 cm (734 SI units) to 306 cm

(1693 SI units) and falls down to 310 cm (597 SI units) where after the values ranges between 350 and 791 up to 402 cm with average of 545 SI units. The  $\chi_{if}$  values show wide variation from 456 cm to 600 cm showing 5 significant peaks at 480 cm (939 SI unit), 510 cm (953 SI unit), 546 cm (1072 SI unit), 572 cm (1401 SI unit) and 582 cm (1070 SI unit). The  $\chi_{if}$  values from 604 cm (464 SI units) to 660 cm (748 SI units) show a significant increase of 144 SI units. Two significant peaks are found to occur at 620 cm (636 SI unit) and 636 cm (623 SI units). In the top 100 cm (Between 700 cm to 800 cm),  $\chi_{if}$  values show a slight variation without any prominent peaks.

The characterisation of each sediment units is done using minimum, maximum and average values of  $\chi_{if}$  SIRM and FMC (Table 7- and Figure 7-). To derive representative values for minimum, maximum and average values of  $\chi_{if}$ , SIRM and FMC for each unit, the values along the unit margins showing wide deviations were not considered. This omission of values avoids skewing of model. The values of  $\chi_{if}$  show a wide variation in maximum and minimum values at Unit 3 (216 to 1693 SI Units). There after a wide variation is observed in lithounit 6, the range goes from 458 to 1401 SI units. Lithounit 1 also shows a moderate variation in the minimum and maximum values that range from 240 to 970 SI units. Whereas, Lithounits 2, 4, 5 and 7 shows a minimum range of variation in the calculated  $\chi_{if}$  value (Lithounit 2- 320 to 696; Lithounit 4- 351 to 667; Lithounit 5- 527 to 940 and Lithounit 7- 476 to 757). Even is a wide variation in the  $\chi_{if}$  value is observed in different units the average value shows a minimum range of variation from 449 to 828 SI units.

In case of SIRM also, the pattern of variation in the maximum and minimum value shows a same trend as  $\chi_{if}$ . The maximum variation is observed in the Unit 3 (2744 to 27372), followed by Unit 6 (5723 to 18361) and Unit 1 (563 to 8653). The minimum variations are observed in Unit 2 (822 to 5703), Unit 4 (3422 to 6956) Unit 5 (6048 to 12258) and Unit 6 (5723 to 18361). However the average value of SIRM shows a variation from 4106 to 10351.

Table 7-: Average magnetic parameters of each lithounit

Lithounit	Depth cm	$\chi_{if}^*$			$\chi_{fd}^*$			SIRM*			FMC*		
		Mini	Max	Av	Mini	Max	Av	Mini	Max	Av	Mini	Max	Av
Unit 7	608-800	476.46	757.19	609.11	0.48	4.67	2.43	563.37	8652.86	6046.87	0.68	9.17	2.76
Unit 6	510-600	457.87	1400.89	827.86	0.21	2.46	1.14	5722.69	18361.03	10350.86	1.59	13.48	4.54
Unit 5	432-492	526.95	939.50	689.02	1.04	1.90	1.55	6048.41	12257.82	8258.84	1.13	12.70	3.90
Unit 4	366-416	350.63	666.68	510.21	1.27	4.12	2.14	3422.19	6955.65	5063.63	2.65	6.52	4.30
Unit 3	162-342	216.24	1693.68	563.05	0.14	4.23	1.93	2743.75	27372.48	7702.32	1.18	18.94	11.17
Unit 2	122-150	320.47	696.92	460.68	1.70	3.19	2.42	844.67	5307.39	4106.17	1.30	4.13	3.00
Unit 1	0-114	240.34	970.16	448.78	1.46	3.52	2.31	3363.57	12240.35	5782.33	9.12	16.57	11.65

\* Anomalous values at the contact of each unit are neglected for the calculation.

The FMC characterise values for lithounits. Lithounit 3 shows wide variation in maximum and minimum values; lithounit 1 shows high average values of FMC; lithounit 5 and 6 have relatively uniform FMC values; lithounit 4 has the minimum deviation with average values similar to lithounit 2, 4, 5, 6 and 7. It is observed from the analysis that lithounit 1 and 3 have high average values of FMC and also wide variation in the maximum and minimum value.

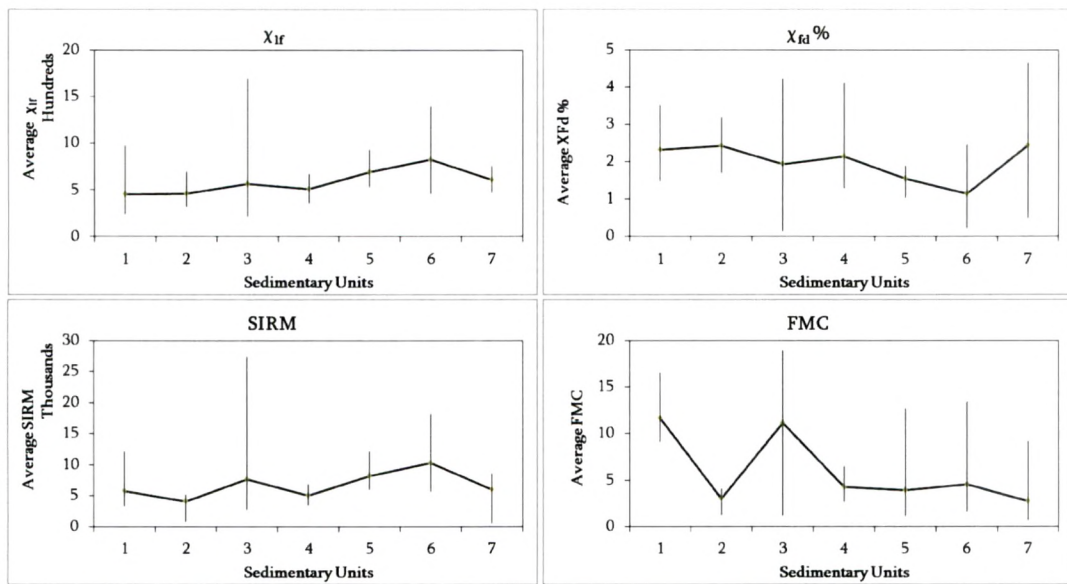


Figure 7-: Minimum, maximum and average values of different parameters

The plot of FMC vs SIRM shows that SIRM values fall within range of 3000 to 9000 SI units with increase in FMC from 0.68 % to 19%, suggesting ferrimagnetic minerals concentrated in the samples have similar magnetic property for lithounits 1, 2, 3, 4, 5 and 7 suggesting similar source for the sediments (Figure 7-). However, the SIRM values for lithounit 6 show a scatter. Within scatter, the samples having FMC below 5%, the SIRM scatters between 6300 and 17000 SI unit whereas for samples having FMC between 10% and 15 %, the SIRM varies between 5900 and 18400 SI unit. The scatter of SIRM could be influenced by role of secondary magnetic mineral

or role of deposition and reworking of primary deposit. However as  $\chi_{fd}$  values show less than 5% variation, this rules out the possible role of secondary magnetic mineral.

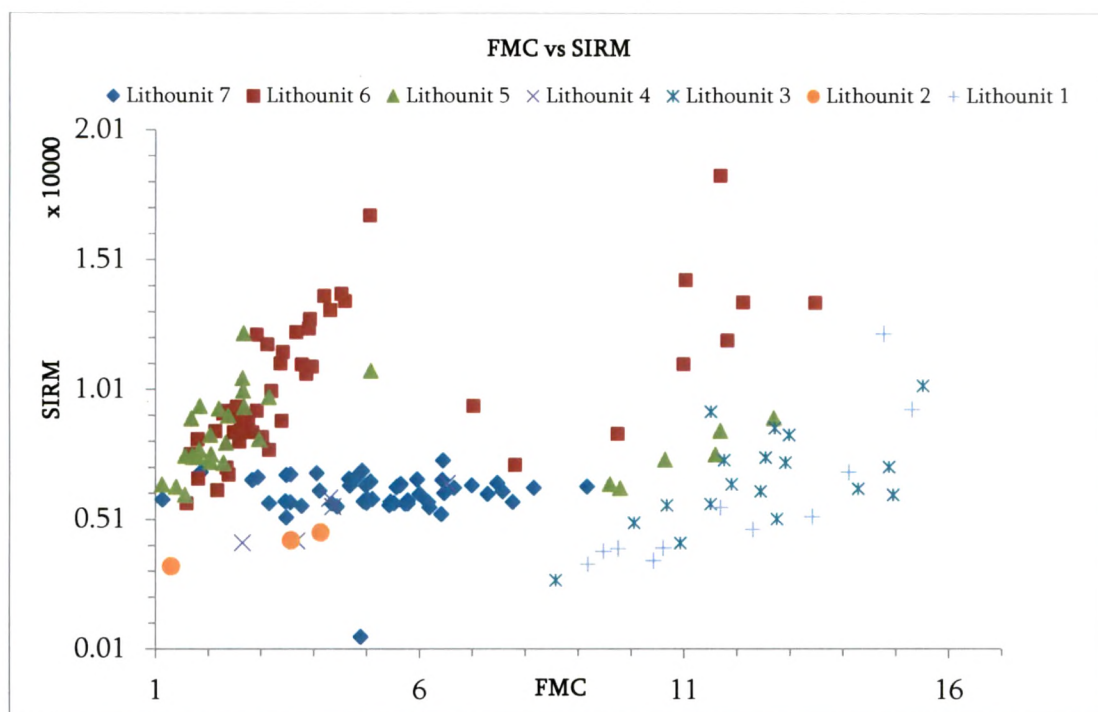


Figure 7-: Plot of ferrimagnetic mineral weight percent verses SIRM

## 7.2 Geochemical Studies

The chemical composition of fluvial sedimentary sequence depends on the provenance, weathering, climate and the subsequent denudational pathways (Johnsson, 1993). The fine facies transported as suspension load gets deposited as overbank or in residual channels acting as natural sediment traps captures provenance and weathering effects over an entire drainage. Therefore, bulk geochemical analyses on bulk samples are highly representative to describe fluvial sediment composition on a basin-wide scale (Ottesen et al., 1989). The chemical records of clastic sediments has been widely used for deciphering provenance (Nath et al., 2000; Singh and Rajamani, 2001b; Singh and Rajamani, 2001a; Pinto et al., 2004; Lee et al., 2005; Sifeta et al.,

2005; Roddaz et al., 2006; Das and Krishnaswami, 2007b; Tripathi et al., 2007; Singh, 2009; Singh, 2010), source area weathering (Nesbitt and Markovics, 1980; Nesbitt and Young, 1982; Nesbitt et al., 1996; Nesbitt and Young, 1996; Nath et al., 2000; Price and Velbel, 2003; Singh et al., 2005; Tripathi et al., 2007), climate (Nesbitt and Young, 1982; Zicheng et al., 2008) and regional uplift in the source region (Sinha et al., 2007b).

### **7.2.1 Methodology**

Geochemical records for seven representative samples, along the depth profile were analysed using ICP AES, a facility made available by Department of Earth Science, Indian Institute of Technology, Powai. The major elements such as Al, Fe, Ti, K, Mg, Mn, Na, P, Ca and Si were quantified.

A standard procedure adopted for geochemical analysis of major elements is summarised. 10 gm of bulk samples was taken using conning and quartering. The fraction is further pulverised to <200 mesh. A 0.250 gm of pulverised sample was mixed with 0.75 g lithium meta-borate,  $\text{LiBO}_2$  (Aldrich Chemical Company) and 0.50 g of lithium tetra borate,  $\text{LiB}_4\text{O}_7$  in a platinum crucible and fused at  $1050^\circ\text{C}$  for 10 min in a muffle furnace. After cooling, the crucible was carefully immersed in 80 ml of 1 M HCl contained in a 150-ml glass beaker and then magnetically stirred for 1 hour until the fusion bead had dissolved completely. Both the stirring bar and dish were removed and rinsed. Sample volume is made to 100ml using standard flask. The solution is further analysed in the ICP- AES (Jobin Vyon Horiba, Ultima-2) using USGS rock standards for calibration. Weight percentage of major elements ( $\text{SiO}_2$ ,  $\text{Al}_2\text{O}_3$ ,  $\text{Fe}_2\text{O}_3$ ,  $\text{CaO}$ ,  $\text{K}_2\text{O}$ ,  $\text{MgO}$ ,  $\text{Na}_2\text{O}$ ,  $\text{TiO}_2$ ,  $\text{MnO}$  and  $\text{P}_2\text{O}_5$ ) were calculated and further used for the analysis.

7.2.2 Results and Discussion

Abundance of oxides percentage for all seven samples, representing different depths, were plotted together to understand the relative variation of along the depth profile (Table 7- and Figure 7-). The plot suggests a relatively high variation in Al<sub>2</sub>O<sub>3</sub>, Fe<sub>2</sub>O<sub>3</sub> and CaO.

Table 7-: Major elemental geochemistry and CIA of samples

Lithounit	7	6	5	4	3	2	1	
Sample no	UCH 60	UCH 120	UCH 160	UCH 210	UCH 280	UCH 330	UCH 400	
Depth (cm)	680-682	560-562	480-482	380-382	240-242	140-142	0-2	
Element (Wt %)	SiO <sub>2</sub>	62.95	64.15	73.47	62.54	84.76	60.55	82.56
	Al <sub>2</sub> O <sub>3</sub>	12.87	10.06	8.25	12.65	5.29	13.28	6.17
	Fe <sub>2</sub> O <sub>3</sub>	11.20	11.07	7.25	10.48	3.20	11.15	3.74
	CaO	5.20	6.74	4.48	6.90	2.95	7.72	3.06
	MgO	2.65	2.83	2.04	2.48	0.99	2.64	1.09
	TiO <sub>2</sub>	2.09	2.25	1.38	1.99	0.54	1.91	0.55
	Na <sub>2</sub> O	1.33	1.26	1.25	1.27	0.84	1.21	1.03
	K <sub>2</sub> O	1.29	1.29	1.65	1.33	1.29	1.11	1.60
	MnO	0.17	0.14	0.09	0.11	0.05	0.15	0.11
	P <sub>2</sub> O <sub>5</sub>	0.13	0.13	0.11	0.13	0.06	0.14	0.08
	LOI	0.11	0.08	0.04	0.13	0.03	0.15	0.03
	CIA	62.20	52.0	52.80	57.12	51.00	56.95	52.01

Table 7-: Correlation coefficient of major elemental concentration

	SiO <sub>2</sub>	Al <sub>2</sub> O <sub>3</sub>	CaO	Fe <sub>2</sub> O <sub>3</sub>	K <sub>2</sub> O	MgO	MnO	Na <sub>2</sub> O	P <sub>2</sub> O <sub>5</sub>	TiO <sub>2</sub>	LOI
SiO <sub>2</sub>	1.00										
Al <sub>2</sub> O <sub>3</sub>	-0.97	1.00									
CaO	-0.94	0.88	1.00								
Fe <sub>2</sub> O <sub>3</sub>	-0.99	0.94	0.91	1.00							
K <sub>2</sub> O	0.56	-0.58	-0.62	-0.54	1.00						
MgO	-0.97	0.89	0.90	0.99	-0.48	1.00					
MnO	-0.82	0.82	0.67	0.84	-0.42	0.80	1.00				
Na <sub>2</sub> O	-0.86	0.81	0.70	0.88	-0.08	0.89	0.78	1.00			
P <sub>2</sub> O <sub>5</sub>	-0.99	0.94	0.90	0.99	-0.47	0.99	0.86	0.91	1.00		
TiO <sub>2</sub>	-0.97	0.89	0.88	0.99	-0.49	0.99	0.79	0.88	0.98	1.00	
LOI	-0.91	0.96	0.89	0.87	-0.72	0.80	0.75	0.64	0.86	0.79	1.00

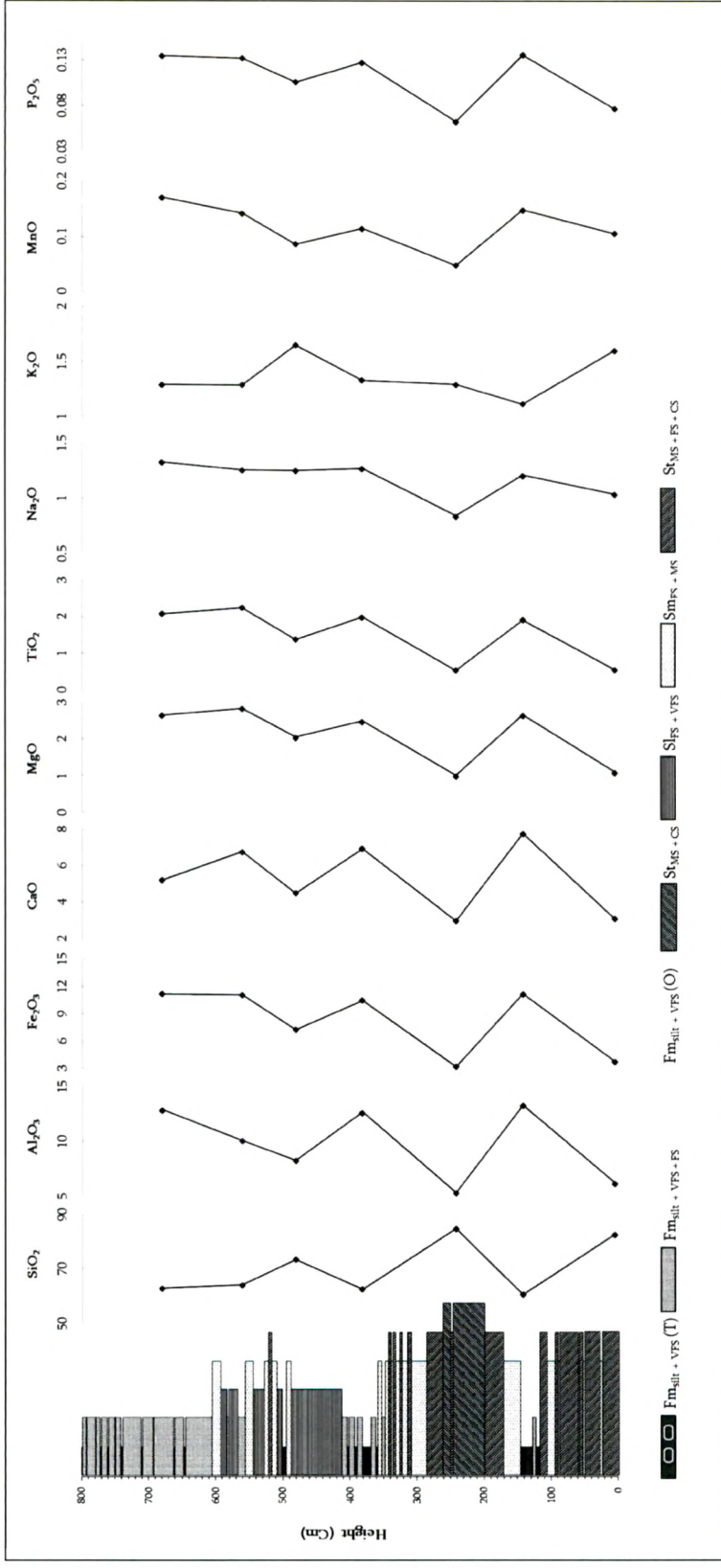


Figure 7:- Depth wise variation of individual major elemental composition along Uchediya sequence compared with sediment subfacies.

The plots further suggest in lithounit 1 and 4 with decrease in SiO<sub>2</sub>, Al<sub>2</sub>O<sub>3</sub>, Fe<sub>2</sub>O<sub>3</sub>, CaO, MgO, and TiO<sub>2</sub> increasing significantly. Whereas along lithounit 1 and 2 increase in SiO<sub>2</sub> values of other oxides decreases.

To understand mutual relation a correlation matrix among the ten major oxides is attempted (Table 7-). It shows SiO<sub>2</sub> (ranges from 62.543 % to 84.764 %) having strong negative correlation (- 0.9889 to - 0.8199 significance) with other 8 oxides (Al<sub>2</sub>O<sub>3</sub>, Fe<sub>2</sub>O<sub>3</sub>, TiO<sub>2</sub>, CaO, Na<sub>2</sub>O, MgO, MnO and P<sub>2</sub>O<sub>5</sub>). However, SiO<sub>2</sub> shows moderate positive correlation with K<sub>2</sub>O (0.558). The correlation matrix further suggests that the oxides namely Al<sub>2</sub>O<sub>3</sub>, Fe<sub>2</sub>O<sub>3</sub>, TiO<sub>2</sub>, CaO, Na<sub>2</sub>O, MgO, MnO and P<sub>2</sub>O<sub>5</sub> have strong positive (0.9937 to 0.66559) among each other except K<sub>2</sub>O with which they show moderate to low negative correlation (-0.6236 to -0.0815). To understand the positive correlation of K<sub>2</sub>O with all other elements, variation of K<sub>2</sub>O is plotted with respect to the depth (Figure 7-). The figure shows that, the percentage of K<sub>2</sub>O is comparatively high in lithounit 1 (140 cm) and lithounit 5 (480 cm).

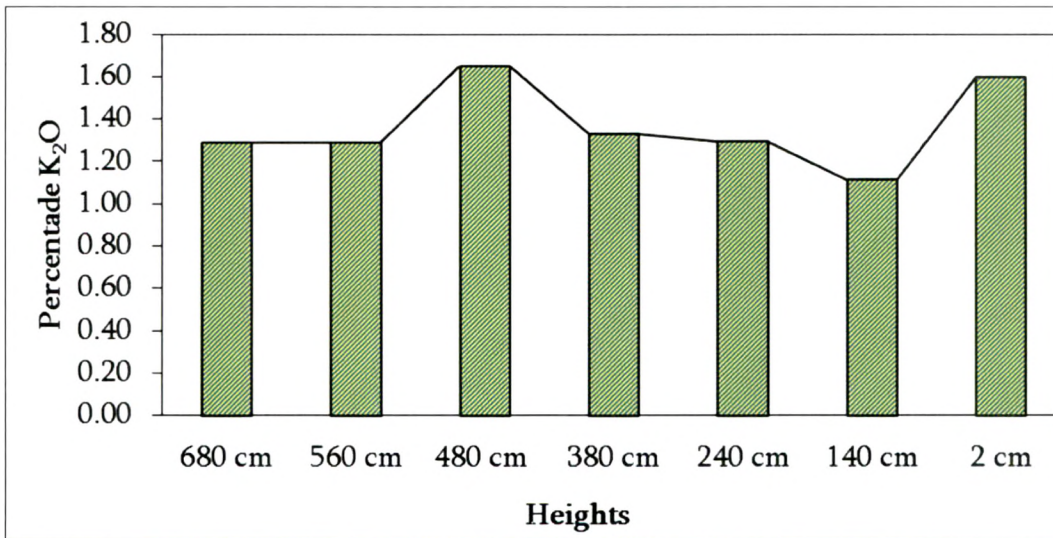


Figure 7-: Concentration of K<sub>2</sub>O plotted against depth shows a relative high concentration at 140 cm depth and 480 cm depth.

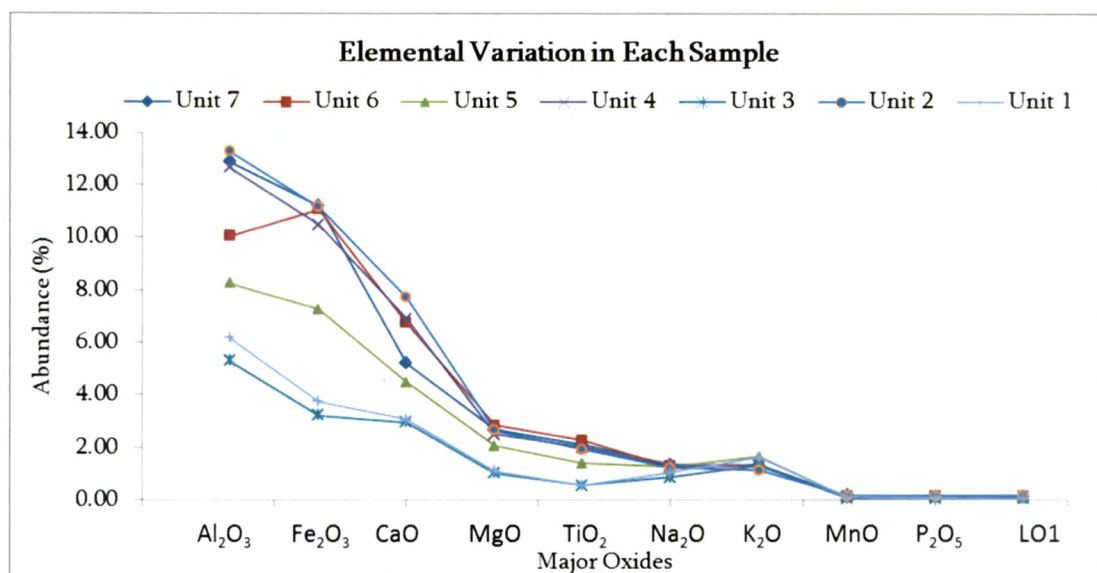


Figure 7-: Concentration of major elements other than Silica plotted for each samples

Figure 7- gives understanding of overall variation in abundance of major oxides. It suggests that the geochemistry of all samples shows similar pattern however in lithounit 6 shows abnormal increase in Fe<sub>2</sub>O<sub>3</sub>.

The variation diagram (major oxides plotted against SiO<sub>2</sub>) shows a linear arrangement of points (Figure 7-). The elements (Al<sub>2</sub>O<sub>3</sub>, TiO<sub>2</sub>, Fe<sub>2</sub>O<sub>3</sub>, Na<sub>2</sub>O, CaO, , MgO, MnO , P<sub>2</sub>O<sub>5</sub>) concentrate in fines (transported as saltation and suspension) for it tends toward 100% SiO<sub>2</sub> whereas element (K<sub>2</sub>O) concentrate in coarse fraction (bed load) for it tend towards 0% SiO<sub>2</sub>.

The binary plot of two immobile elements Al<sub>2</sub>O<sub>3</sub> vs Fe<sub>2</sub>O<sub>3</sub>, Al<sub>2</sub>O<sub>3</sub> vs TiO<sub>2</sub> and Fe<sub>2</sub>O<sub>3</sub> vs TiO<sub>2</sub> (Figure 7-) shows three distinct groups. Whereas, the plots of mobile elements K<sub>2</sub>O vs Na<sub>2</sub>O, K<sub>2</sub>O vs P<sub>2</sub>O<sub>5</sub>, CaO vs P<sub>2</sub>O<sub>5</sub> and CaO vs Na<sub>2</sub>O show scatter as these elements are likely to get fractionated during denudational processes.

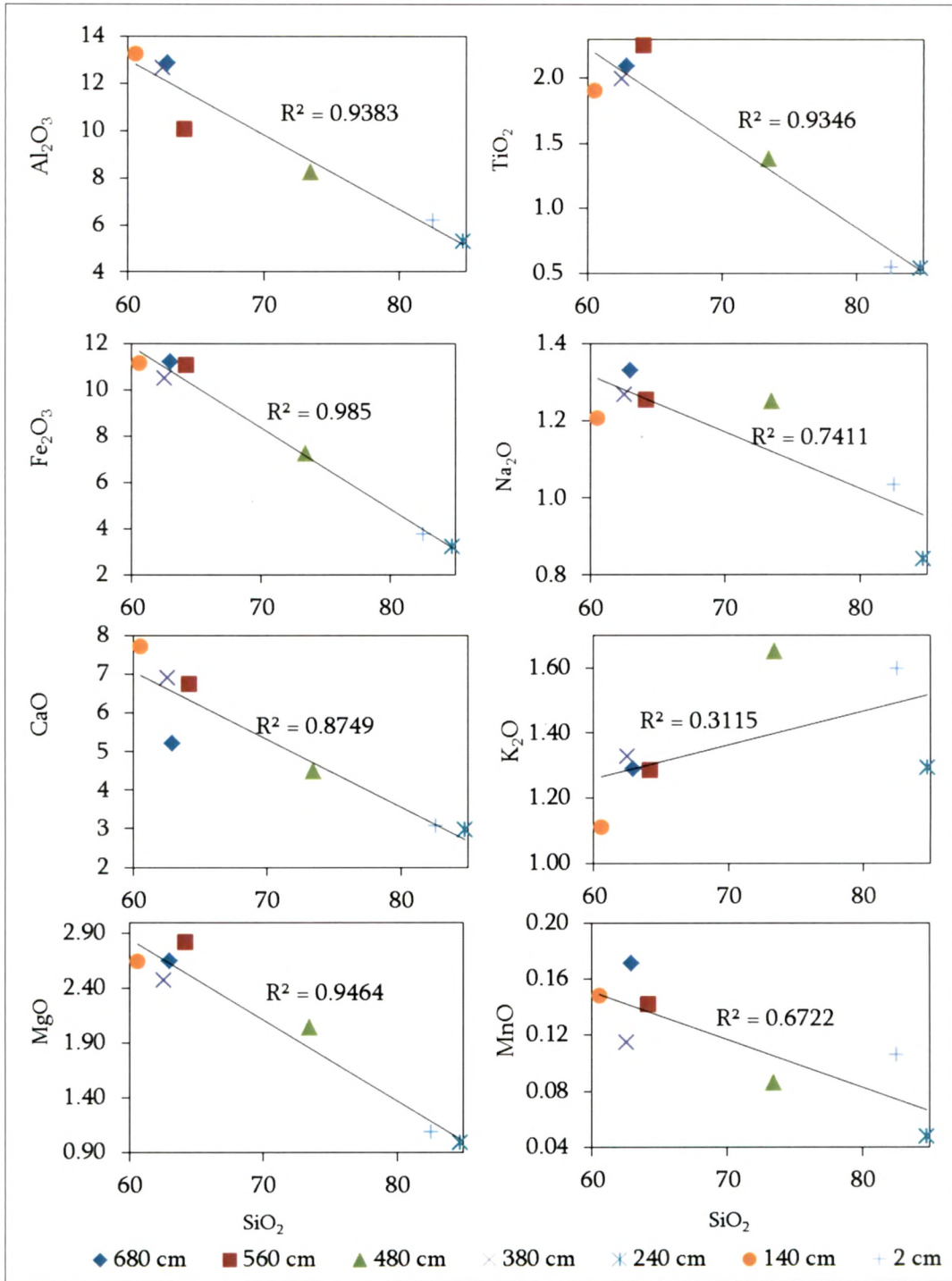


Figure 7-: Variation diagram of major oxides with respect to SiO<sub>2</sub>

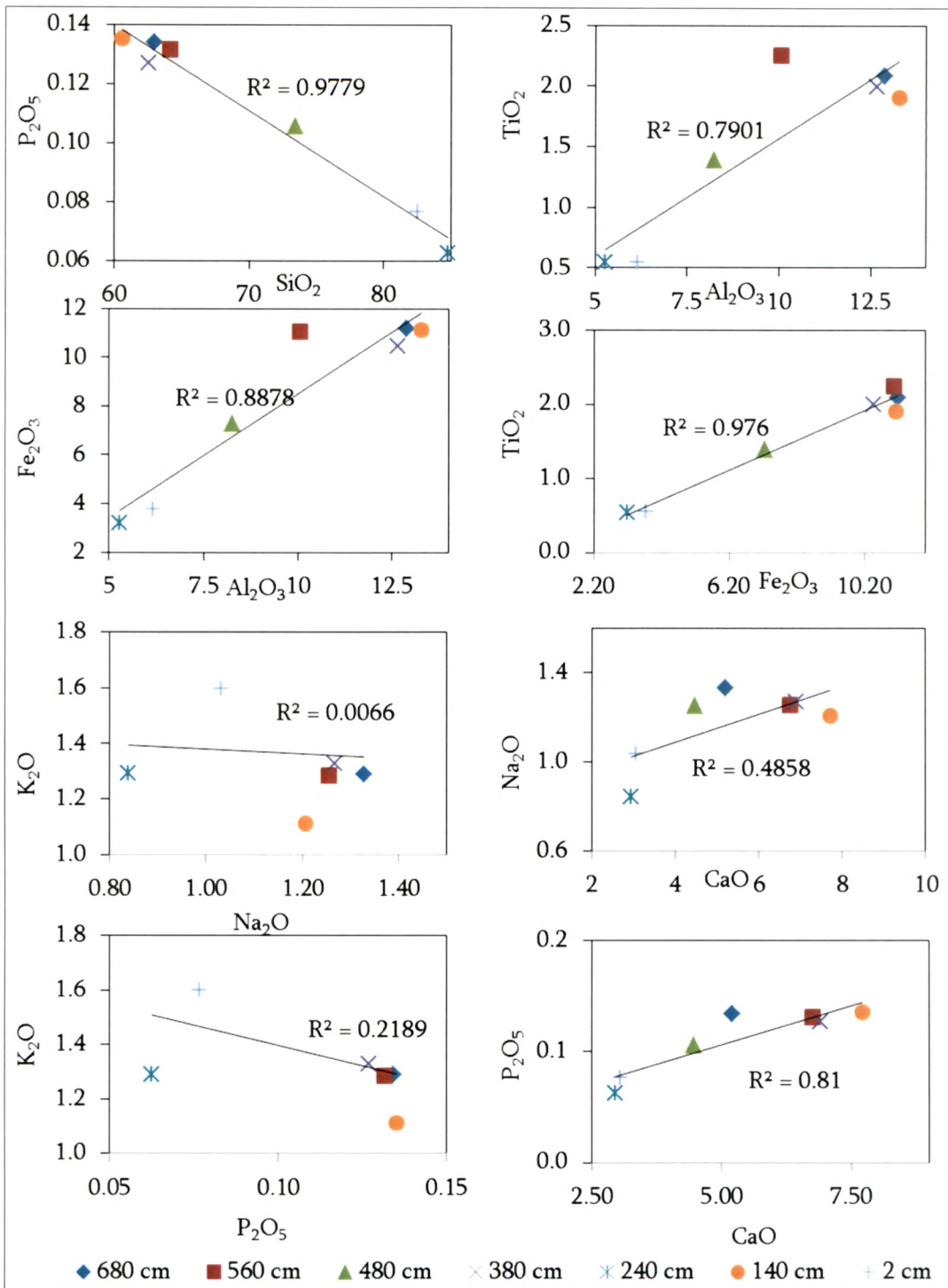


Figure 7-: Bivariant plot capturing relative variation between major oxides.

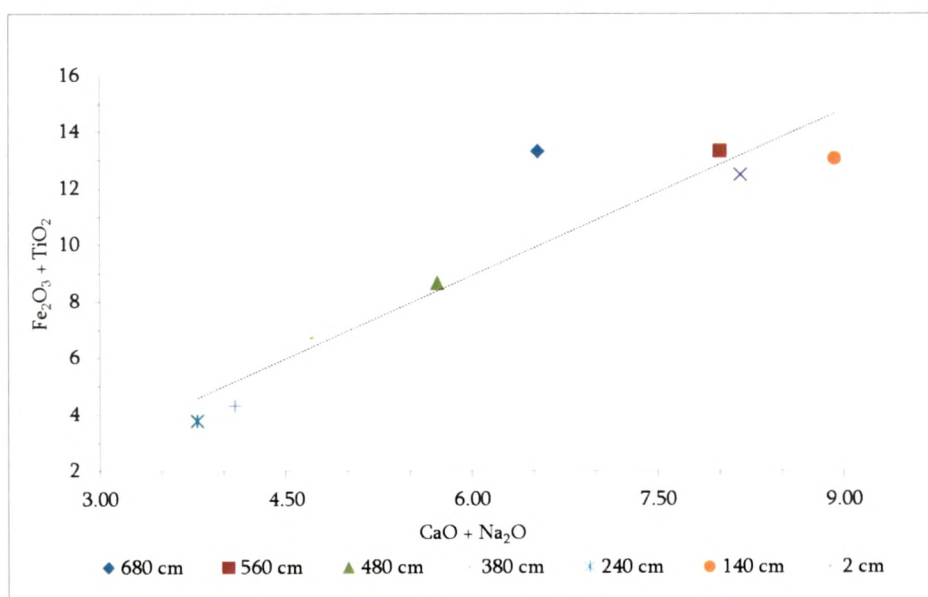


Figure 7-: Plots of CaO+Na<sub>2</sub>O vs Fe<sub>2</sub>O<sub>3</sub>+TiO<sub>2</sub>

The plots of CaO+Na<sub>2</sub>O vs Fe<sub>2</sub>O<sub>3</sub>+TiO<sub>2</sub> were plotted to understand the possible source of iron bearing minerals. The plot shows that iron minerals (Fe<sub>2</sub>O<sub>3</sub>+TiO<sub>2</sub>) have positive trend with Feldspar (CaO+Na<sub>2</sub>O), indicate Basaltic terrain as a source (Figure 7-).

An estimation of the degree of chemical weathering of each lithounit is obtained by calculating the Chemical Index of Alteration (CIA-Table 7-) (Nesbitt and Young, 1982). These parameters have extensively used by different researchers to understand the chemical maturity and province weathering (Singh and Rajamani, 2001a; Lee et al., 2005; Das and Krishnaswami, 2007a; Tripathi et al., 2007; Manikyamba et al., 2008; Oh et al., 2008; Roy et al., 2008; Singh, 2009; Singh, 2010). The CIA values of fresh rocks and minerals are consistently near 50. The samples with CIA values below 60 display low chemical weathering, between 60 and 80 indicate moderate chemical weathering and more than 80 exhibit extreme chemical weathering (Fedo et al., 1995). All lithounits except lithounit 7 indicate a low chemical weathering of 51 to 57, whereas, lithounit 7 indicates a moderate chemical weathering of the sediments (62.20). Low weathering/diagenesis of the sequence is also suggested by significantly low value of  $\chi_{rd}$ %.

### **7.3 Inferences**

- 1 The magnetic susceptibility of all the sediments vary from 216-1693  $10^{-6} \text{ m}^3\text{kg}^{-1}$  and standard deviation of 205  $10^{-6} \text{ m}^3\text{kg}^{-1}$ , indicate that the sediment is composed of relatively high magnetic susceptible minerals.
- 2 A low dependency value (1.9 to 4.67 %) of all the sediments shows that the sediment is composed of single domain magnetic grains.
- 3 Each unit in the vertical section is characterized by a break in the magnetic properties whereas the average value of each unit shows a minimum variation indicates uniform source for the sediments.
- 4 Major element geochemistry of 7 represented samples from each lithounit shows a minor compositional variation.
- 5 Silica shows a well negative correlation with all other elements other than  $\text{K}_2\text{O}$ . With  $\text{K}_2\text{O}$  (0.56) which shows a positive correlation.
- 6 Binary plots of mobile and immobile elements show that lithounit 5 is chemically distinct from other lithounits.
- 7 Chemical index of alteration indicate that the sediments are chemically unaltered except unit 7 which shows a low chemical weathering.